

Field induced changes in the ring/chain equilibrium of hydrogen bonded structures: 5-methyl-3-heptanol

Amanda R. Young-Gonzales, and Ranko Richert

Citation: *The Journal of Chemical Physics* **145**, 074503 (2016); doi: 10.1063/1.4961022

View online: <http://dx.doi.org/10.1063/1.4961022>

View Table of Contents: <http://aip.scitation.org/toc/jcp/145/7>

Published by the [American Institute of Physics](#)

Articles you may be interested in

[Dynamics of glass-forming liquids. XX. Third harmonic experiments of non-linear dielectric effects versus a phenomenological model](#)

The Journal of Chemical Physics **145**, 064510 (2016); 10.1063/1.4960620

[Dynamics of glass-forming liquids. XIX. Rise and decay of field induced anisotropy in the non-linear regime](#)

The Journal of Chemical Physics **143**, 104504 (2015); 10.1063/1.4929988

[Relaxation time and excess entropy in viscous liquids: Electric field versus temperature as control parameter](#)

The Journal of Chemical Physics **146**, 064501 (2017); 10.1063/1.4975389

[Dynamics of glass-forming liquids. XVIII. Does entropy control structural relaxation times?](#)

The Journal of Chemical Physics **142**, 044504 (2015); 10.1063/1.4906191

[Communication: Supramolecular structures in monohydroxy alcohols: Insights from shear-mechanical studies of a systematic series of octanol structural isomers](#)

The Journal of Chemical Physics **141**, 101104 (2014); 10.1063/1.4895095

[Linear and nonlinear dielectric theory for a slab: The connections between the phenomenological coefficients and the susceptibilities](#)

The Journal of Chemical Physics **145**, 084105 (2016); 10.1063/1.4961225



**COMPLETELY
REDESIGNED!**



**PHYSICS
TODAY**

Physics Today Buyer's Guide
Search with a purpose.

Field induced changes in the ring/chain equilibrium of hydrogen bonded structures: 5-methyl-3-heptanol

Amanda R. Young-Gonzales and Ranko Richert

School of Molecular Sciences, Arizona State University, Tempe, Arizona 85287-1604, USA

(Received 24 June 2016; accepted 1 August 2016; published online 16 August 2016)

Using non-linear dielectric techniques, we have measured the dynamics of 5-methyl-3-heptanol at a temperature at which the Kirkwood correlation factor g_K indicates the coexistence of ring- and chain-like hydrogen-bonded structures. Steady state permittivity spectra recorded in the presence of a high dc bias electric field (17 MV/m) reveal that both the amplitude and the time constant are increased by about 10% relative to the low field limit. This change is attributed to the field driven conversion from ring-like to the more polar chain-like structures, and a direct observation of its time dependence shows that the ring/chain structural transition occurs on a time scale that closely matches that of the dielectric Debye peak. This lends strong support to the picture that places fluctuations of the end-to-end vector of hydrogen bonded structures at the origin of the Debye process, equivalent to fluctuations of the net dipole moment or g_K . Recognizing that changes in the ring/chain equilibrium constant also impact the spectral separation between Debye and α -process may explain the difference in their temperature dependence whenever g_K is sensitive to temperature, i.e., when the structural motifs of hydrogen bonding change considerably. *Published by AIP Publishing.* [<http://dx.doi.org/10.1063/1.4961022>]

I. INTRODUCTION

Hydrogen bonds play a significant role regarding the properties of liquids such as water, alcohols, and amides. The dielectric properties of these materials have been studied extensively with the goal of understanding the role of the hydrogen bonds regarding the structure and dynamics in these liquids.¹ Many monohydroxy alcohols,^{2,3} various amides,^{4–6} and possibly water^{7,8} belong to a class of liquids for which the prominent dielectric relaxation process does not reflect the typical signatures of structural relaxation, such as the heat capacity step,^{9–11} shear mechanical relaxation,^{12,13} or density-density correlation functions.¹⁴ Another common feature of these liquids is the Debye type nature of its prominent dielectric loss peak, which is retained even at the glass-transition for those cases where crystallization can be avoided.¹ It is generally accepted that hydrogen bonding is at the origin of these particular properties of this class of liquids. In many cases, e.g., 1-propanol, chain structures connected by hydrogen bonding develop, especially at lower temperatures.¹⁵

The preferred supramolecular structures that develop through hydrogen bonding will depend on the structure of the compound involved. Steric hindrance can lead to a higher population of ring-like structures or inhibit intermolecular hydrogen bonding altogether.^{16,17} In this respect, a series of isomeric octyl alcohols has received considerable attention. A number of these isomers have been studied by Dannhauser,¹⁸ revealing that the position of a methyl group can modify the Kirkwood-Fröhlich correlation factor g_K to a large extent. This factor gauges the strength of the effective dipole moment relative to the molecular dipole,¹⁹

$$g_K = \frac{\mu_{eff}^2}{\mu^2} = 1 + z \langle \cos \theta \rangle, \quad (1)$$

which results from orientational correlation of dipole moments. Here, z is the average number of neighbors and $\langle \cos \theta \rangle$ is the averaged cosine of the angle between the dipoles. The more parallel dipole alignment of chain structures leads to an enhancement of μ_{eff}/μ and g_K with a concomitant increase of the dielectric constant, ϵ_s . By contrast, ring-like dipole structures involve anti-parallel alignment that leads to g_K values below unity. The case of $g_K \approx 1$ could indicate either uncorrelated dipoles or the coexistence of chains ($g_K > 1$) and rings ($g_K < 1$).¹⁵

Among the isomeric octyl alcohol series, 5-methyl-3-heptanol (5M3H) is particularly interesting because its net g_K value changes from above to below unity across a relatively small temperature window.¹⁸ The dielectric loss spectra and the temperature variation of g_K in this range of interest are shown in Fig. 1. This behavior suggests that ring- and chain-like structures have similar free energies in 5M3H around $T = 200$ K and that the equilibrium constant for the ring and chain population is not far from unity.²⁰ Because chain structures are much more dipolar than rings, it is expected that this equilibrium may be influenced by an external electric field, which was the basis for recent high ac field dielectric studies of 5M3H and related liquids.^{20,21} The conclusion from those experiments was that the electric field does enhance the relaxation amplitudes via an increase of g_K , but the effect fades at higher frequencies because the ring/chain conversion requires a time scale that is near that of the Debye process. Accordingly, the relaxation amplitudes return to the low field values for frequencies above those of the Debye peak loss maximum.

The present study revisits 5M3H in terms of a time resolved dielectric study in which the ring/chain equilibrium is altered through high dc-bias (opposed to ac) electric fields. In the steady state case and for a field of $E_B = 171$ kV cm⁻¹,

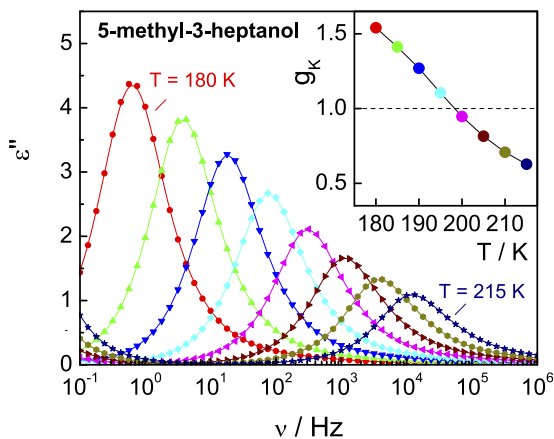


FIG. 1. Low field dielectric loss spectra of 5-methyl-3-heptanol for temperatures from 180 K to 210 K in steps of 5 K. The inset shows the Kirkwood correlation factor, g_K , of 5M3H for the same temperature range. Data taken from Refs. 20 and 21.

we observe a relative change of the relaxation amplitude of $\Delta_E \ln \varepsilon_D = +11.0\%$ and a relative change of the time constant of $\Delta_E \ln \tau_D = +12.6\%$ concerning the Debye process. These two quantities are not only similar in their steady state magnitude but also follow the same time dependence that closely matches the Debye time constant, τ_D . The result is a cancellation effect that renders the high frequency permittivity practically field invariant. The observations suggest that a field induced ring-to-chain conversion not only increases the net Kirkwood correlation factor g_K and thus $\Delta\varepsilon$ but also slows down the dynamics associated with the Debye process. This correlation explains a change in the spectral separation between Debye time and the primary structural relaxation whenever g_K changes, i.e., usually as a function of temperature.

II. EXPERIMENTS

The compound 5-methyl-3-heptanol (5M3H, purity unspecified) was purchased from Sigma-Aldrich and used as received. Low field impedance measurements were obtained using a Solartron SI-1260 gain/phase analyzer with a Mestec DM-1360 transimpedance amplifier. Low field measurements are used to verify sample properties and to obtain an accurate electrode spacing through the comparison of the relaxation amplitude ($\Delta\varepsilon$) to reference data. This is necessary because at electrode spacer thicknesses of around 10 μm , deviations between actual and nominal distance are common.

The high field cell capacitor consists of two spring loaded polished stainless steel electrodes (17 mm and 20 mm), separated by a 13 μm thick Kapton ring that leaves an inner area of 14 mm diameter for the sample. For all measurements, the cell is mounted onto the cold stage of a closed cycle He-refrigerator cryostat Leybold RDK 6-320 with Coolpak-6200 compressor. A Lakeshore Model 340 temperature controller stabilizes the temperature within several mK. High bias field experiments aimed at steady state results are performed using a Solartron 1260 gain/phase analyzer, with the voltage amplified

by a Trek PZD-350 amplifier. The voltage at the sample is measured at the “V1” input of the SI-1260 using the voltage monitor output of the Trek PZD-350 amplifier. The current is recorded as the voltage drop across an RC network shunt, the impedance of which is designed to increase from 250 Ω at 10^4 Hz to 300 k Ω at 1 Hz in order to counteract the reduced current levels at low frequencies. The shunt output is ac-coupled ($RC = 0.12$ s) to a buffer amplifier that protects the system from sample failure. The output of that buffer is analyzed via the “V2” input of the SI-1260. For each frequency, the system is programmed to perform 15 measurements with the bias field E_B on, followed by 15 measurements with no bias, where each measurement integrates the signal for the greater of 1 s or 18 periods. This protocol is meant to capture steady state impedance values at the high field, while avoiding excessive exposure to high fields and providing ample recovery time between high field measurements. Due to the lack of time resolution in this acquisition mode, the results could deviate from true steady state values.

Time resolved measurements are performed as described in detail earlier.²² A Stanford Research Systems DS-345 programmable wave form generator supplies the voltage waveform, which is amplified by a factor of 100 using a Trek PZD-350 high voltage amplifier. The programmed sinusoidal waveforms, $V(t) = V_B + V_0 \sin(\omega t)$, consist of an integer number of periods, where the bias voltage V_B is applied only for some of the periods. In this case, $V_B/V_0 = 4$, so that the amplitude of the ac field component is practically in the regime of linear responses. The voltage and current ($R = 3$ k Ω shunt) signals are recorded using a Nicolet Sigma 100 digitizing oscilloscope that averages over 5000 waveform repetitions. In order to eliminate the direct polarization response to applying or removing the bias field, all signal traces refer to an average of two measurements: one with positive bias voltage and one with negative bias voltage of the same magnitude. These averaged voltage $V(t)$ and current $I(t)$ traces are subject to period-by-period Fourier analysis, yielding the amplitudes (A) and phases (φ) of the voltage (A_V, φ_V) and current (A_I, φ_I) for each period. The effect of the high bias field is quantified by the out-of-phase “permittivity” evaluated for each measured period using

$$e'' = \left| \frac{A_I \cos(\varphi_I - \varphi_V)}{\omega A_V C_0} \right|, \quad (2)$$

where C_0 is the geometric capacitance of the cell, nominally $C_0 = 105$ pF. The notation e'' is used instead of ε'' because this quantity changes with time in a non-equilibrium situation where permittivity ε is not properly defined.

III. RESULTS

The quasi-steady state effects resulting from the high dc bias field of $E_B = 171$ kV cm^{-1} are presented graphically as the relative difference of the high and low field spectra of permittivity in Figs. 2 and 3. The storage component of the permittivity in Fig. 2 is represented as $(\varepsilon'_{hi} - \varepsilon'_{lo})/(\varepsilon'_{lo} - \varepsilon_\infty)$, where the infinite frequency dielectric constant, ε_∞ , is subtracted because electronic polarizability is considered field

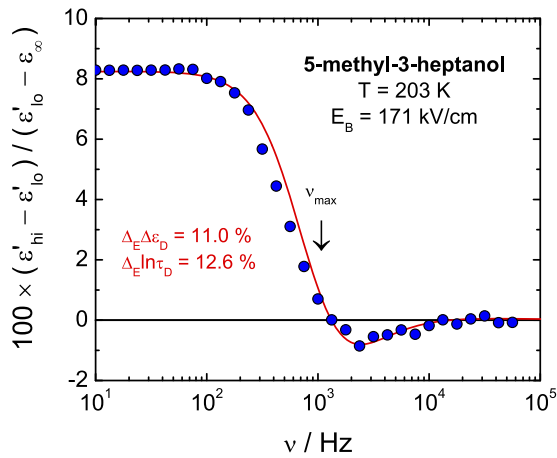


FIG. 2. Symbols represent the experimental field induced ($E_B = 171 \text{ kV cm}^{-1}$) steady state spectra of the relative change of the real part of permittivity, $(\epsilon'_{\text{hi}} - \epsilon'_{\text{lo}})/(\epsilon'_{\text{lo}} - \epsilon_{\infty})$, for 5M3H at $T = 203 \text{ K}$. The value of ϵ_{∞} is subtracted from the ϵ' data because it is considered field invariant. The line is calculated based on ϵ'_{lo} determined from an HN fit to the low field data and with ϵ'_{hi} given by the same fit but with the Debye amplitude and time constant modified according to $\Delta_E \ln \epsilon_D = 11.0\%$ and $\Delta_E \ln \tau_D = 12.6\%$, respectively. The arrow indicates the frequency position of the low field loss peak, ν_{max} .

invariant. The main feature of Fig. 2 is the 8% increase of the quantity $(\epsilon' - \epsilon_{\infty})$, which fades towards higher frequencies, similar to previous observations.^{20,21} The dielectric loss counterpart is shown as $(\epsilon''_{\text{hi}} - \epsilon''_{\text{lo}})/\epsilon''_{\text{lo}}$ in Fig. 3. These changes in ϵ'' are more pronounced, but also approach practically zero for frequencies that exceed $10 \times \nu_{\text{max}}$, where ν_{max} is the low field loss peak position (indicated by arrows in both figures).

A time resolved measurement of $(\epsilon''_{\text{hi}} - \epsilon''_{\text{lo}})/\epsilon''_{\text{lo}}$ at the frequency $\nu = 1.0 \text{ kHz}$ is provided in Fig. 4. This measurement frequency is selected to closely match that of the loss peak, i.e., $\nu_{\text{max}} = 1075 \text{ Hz}$ at this temperature of $T = 203 \text{ K}$. In this case, a steady state plateau value of 8.75% is reached

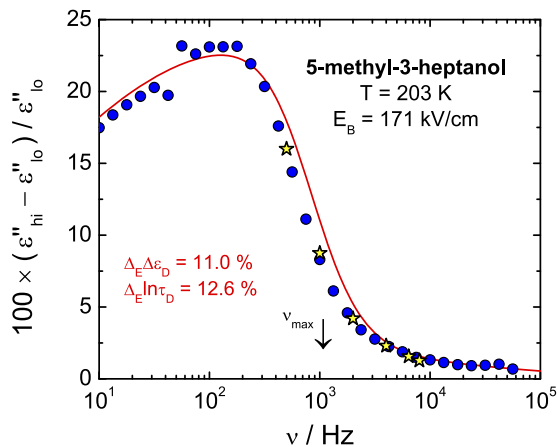


FIG. 3. Symbols represent the experimental field induced ($E_B = 171 \text{ kV cm}^{-1}$) steady state spectra of the relative change of the dielectric loss, $(\epsilon''_{\text{hi}} - \epsilon''_{\text{lo}})/\epsilon''_{\text{lo}}$, for 5M3H at $T = 203 \text{ K}$. The line is calculated based on ϵ''_{lo} determined from an HN fit to the low field data and with ϵ''_{hi} given by the same fit but with the Debye amplitude and time constant modified according to $\Delta_E \ln \epsilon_D = 11.0\%$ and $\Delta_E \ln \tau_D = 12.6\%$, respectively. The arrow indicates the frequency position of the low field loss peak, ν_{max} . Stars show the steady state plateau values from the time resolved experiments.

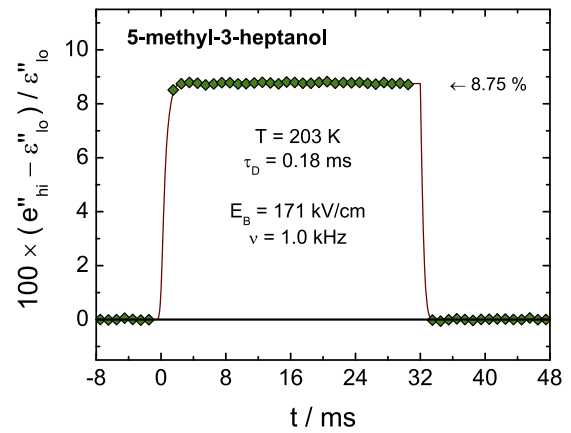


FIG. 4. Symbols represent the experimental field induced ($E_B = 171 \text{ kV cm}^{-1}$) relative change of the dielectric “loss,” $(\epsilon''_{\text{hi}} - \epsilon''_{\text{lo}})/\epsilon''_{\text{lo}}$, versus time for 5M3H at $T = 203 \text{ K}$ for a frequency $\nu = 1 \text{ kHz}$ ($\approx \nu_{\text{max}}$). The line is calculated based on a squared exponential time dependence, $A \times [1 - \exp(-t/\tau)]^2$ and $A \times \exp(-t/\tau)^2$ with $A = 8.75\%$ and $\tau = 0.24 \text{ ms}$.

after few ms. In this time resolved technique, the temporal resolution is limited to one period, equivalent to 1 ms in the case of Fig. 4. Expectedly, the plateau level of 8.75% is consistent with the change seen in Fig. 2 at $\nu = 1.0 \text{ kHz}$. Similar measurements performed at higher frequencies with $\nu > \nu_{\text{max}}$ are compiled in Fig. 5. The resulting steady state values for $\nu = 4.0, 6.4,$ and 8.0 kHz indicate field induced increases in ϵ'' of 2.30%, 1.56%, and 1.27%, respectively. All plateau values observed by time resolved experiments are

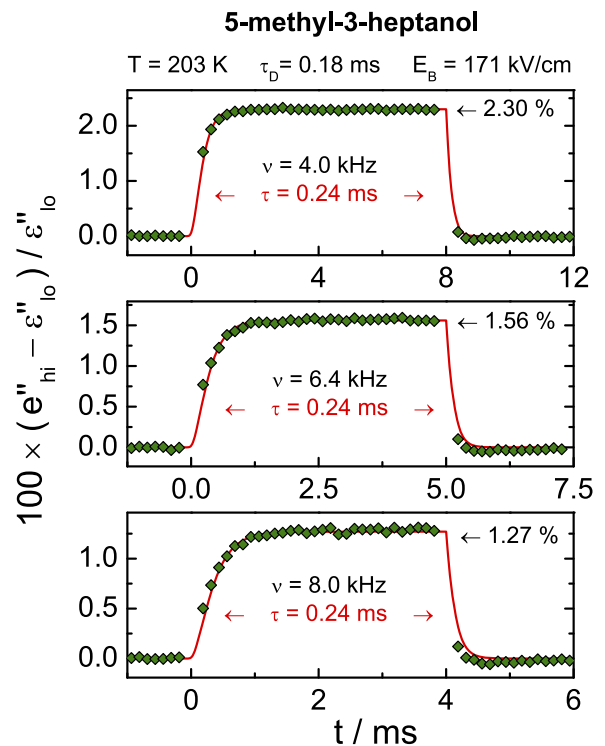


FIG. 5. Symbols represent the experimental field induced ($E_B = 171 \text{ kV cm}^{-1}$) relative change of the dielectric “loss,” $(\epsilon''_{\text{hi}} - \epsilon''_{\text{lo}})/\epsilon''_{\text{lo}}$, versus time for 5M3H at $T = 203 \text{ K}$ for the frequencies $\nu = 4.0, 6.4,$ and 8.0 kHz ($> \nu_{\text{max}}$). The lines are calculated based on a squared exponential time dependence, $A \times [1 - \exp(-t/\tau)]^2$ and $A \times \exp(-t/\tau)^2$ with A equal to the respective plateau value (as indicated) and with a common value of $\tau = 0.24 \text{ ms}$.

included as stars in the spectrum of Fig. 3, with the agreement confirming the steady state nature of the spectrum.

The quadratic field dependence of the steady state effect has been verified by determining $\Delta_E \ln \tau_D$ at different fields. The results are $\Delta_E \ln \tau_D = 2.8\%$ at $E_B = 82 \text{ kV cm}^{-1}$ and $\Delta_E \ln \tau_D = 12.6\%$ at $E_B = 171 \text{ kV cm}^{-1}$. From these values, a power law relation with power $\log(12.6/2.8)/\log(171/82) = 2.04$ is found, consistent with the expected quadratic field dependence. We also note that qualitatively analogous results were found for mixtures of 5M3H or 4-methyl-3-heptanol with 1-propanol, where the propanol content was around 5%–10% by weight.

IV. DISCUSSION

The dc field induced changes of the quantity $(\varepsilon' - \varepsilon_\infty)$ observed in Fig. 2 are highly reminiscent of what had been seen earlier for 5M3H using high amplitude (bias free) ac fields.^{20,21} As in the previous studies, this field driven increase of $\Delta\varepsilon$ is understood as the result of the high field shifting the ring/chain equilibrium constant, $K_{r/c}$, towards the more polar species, i.e., favoring the chains and thus increasing the net g_K . In the present case, however, the disappearance of the amplitude enhancement for $\nu > \nu_{\max}$ cannot be attributed to the frequency exceeding the rate at which $\varepsilon'(\omega)$ can change via g_K . The reason for this notion is that the alternating field component, E_0 , is within the regime of linear response (applied electric field is $E(t) = E_B + E_0 \sin(\omega t)$ with $E_B/E_0 = 4$) and thus has practically no impact on the ring/chain equilibrium, which now is only a matter of the static high field E_B . As a result, a different explanation for the frequency dependence of the non-linear effects must be found.

In order to rationalize the steady state results of Figs. 2 and 3, a quantitative analysis of these spectra is required. To this end, the low field loss spectra (see Fig. 1) are fit with the sum of a Debye type and a Havriliak-Negami (HN) type dielectric process.²³ These fits employ the permittivity function,

$$\varepsilon^*(\omega) = \varepsilon_\infty + \frac{\Delta\varepsilon_D}{1 + i\omega\tau_D} + \frac{\Delta\varepsilon_\alpha}{[1 + (i\omega\tau_\alpha)^\alpha]^\gamma} \quad (3)$$

where ε_∞ is the dielectric constant in the high frequency limit, and $\Delta\varepsilon_D$ and τ_D are the amplitude and time constant associated with the Debye process. The additional small signature of the primary (α) relaxation mode is characterized by its amplitude $\Delta\varepsilon_\alpha$, its time constant τ_α , and the exponents α and γ that define the symmetric and asymmetric broadening of the loss peak, respectively. Fits to the low field permittivity curves define ε_∞ , ε'_{10} , and ε''_{10} . Results for ε'_{hi} and $\varepsilon''_{\text{hi}}$ are obtained by allowing $\Delta\varepsilon_D$ and τ_D to be modified by the high field, whereas all parameters associated with the α -process are considered field invariant. The two field dependent quantities, $\Delta\varepsilon_D$ and τ_D , are adjusted for a best fit to the experimental data for $(\varepsilon'_{\text{hi}} - \varepsilon'_{10})/(\varepsilon'_{10} - \varepsilon_\infty)$ in Fig. 2 and $(\varepsilon''_{\text{hi}} - \varepsilon''_{10})/\varepsilon''_{10}$ in Fig. 3. It turns out that the field effect on both the storage and the loss components can be described by the same parameters, with the field induced changes being quantified by $\Delta_E \ln \Delta\varepsilon_D = +11.0\%$ and $\Delta_E \ln \tau_D = +12.6\%$.

This 11% increase of $\Delta\varepsilon_D$ amounts to an 8.2% change of the total $\Delta\varepsilon = \Delta\varepsilon_D + \Delta\varepsilon_\alpha$, which appears as low frequency plateau level in Fig. 2. The curves calculated on the basis of the $\Delta_E \ln \Delta\varepsilon_D$ and $\Delta_E \ln \tau_D$ values are included as solid lines in both Figs. 2 and 3. The coincidence of these fits with the experimental data validates that the field dependence of $\Delta\varepsilon_D$ and τ_D is sufficient to describe how the permittivity is modified by a static field of high amplitude.

In the previous studies of 5M3H based upon high amplitude ac fields,^{20,21} the parameter $\Delta\varepsilon_D$ was the only variable considered to be sensitive to the high field. Presently, we find not only that both Debye peak parameters, $\Delta\varepsilon_D$ and τ_D , change with E_B but also that their relative changes are similar in magnitude. As a result, the field driven increase in peak amplitude and shift of the peak position to lower frequencies lead to a near perfect cancellation of the two effects, so that the high frequency regime of the permittivity appears field invariant. This cancellation feature does not seem to be accidental in the case of 5M3H, as the same behavior can be observed for mixtures of 5M3H or 4M3H with 1-propanol. Therefore, the basis for deriving a time scale for the ring-to-chain conversion from the frequency dependence of the earlier^{20,21} high ac field experiments is no longer justified.

In order to assess the time scale of the ring/chain population to reach equilibrium after a change in the dc field, we turn to the time resolved experiments at selected frequencies shown in Figs. 4 and 5. The case of $\nu = 1.0 \text{ kHz}$ in Fig. 4 picks up the time dependence of the amplitude change, $\Delta_E \ln \Delta\varepsilon_D$, selectively, because a lateral shift along the frequency axis remains undetected at the peak frequency ν_{\max} , where $\partial \ln \varepsilon / \partial \ln \nu = 0$. On the other hand, the limited time resolution of 1 ms is insufficient for resolving the dynamics. At the higher frequencies of Fig. 5, the changes are resolved across several periods in time, but these curves involve both $\Delta_E \ln \Delta\varepsilon_D$ and $\Delta_E \ln \tau_D$. In Fig. 5 it is particularly the $\nu = 8 \text{ kHz}$ case that reveals the asymmetric response to applying and removing the field, where the fall time appears to be much shorter than the rise behavior.

In analogy to an earlier analysis of time-resolved nonlinear effects,^{24,25} we recognize that the steady state levels of $\Delta_E \ln \Delta\varepsilon_D$ and $\Delta_E \ln \tau_D$ depend quadratically on the field E_B . Because the deviations from the $P(E_B)$ linearity are still quite small, a reasonable approximation to the time dependence of the nonlinear effect is the proportionality to the squared time dependent polarization, P , where $P(t)$ is an exponential. Therefore, the curves in Fig. 5 are assumed to follow $\phi(t) \times [e''_{\text{hi}}(t \rightarrow \infty) - \varepsilon''_{10}]/\varepsilon''_{10}$, with

$$\phi(t) = \begin{cases} \left(1 - e^{-(t-t_{\text{on}})/\tau}\right)^2, & t_{\text{on}} \leq t \leq t_{\text{off}} \\ \left(e^{-(t-t_{\text{off}})/\tau}\right)^2, & t \geq t_{\text{off}} \end{cases} \quad (4)$$

where t_{on} and t_{off} are the times at which the field E_B is applied and removed, respectively. For the four frequencies of Figs. 4 and 5, the solid lines demonstrate that Eq. (4) with a common time constant of $\tau = 0.24 \text{ ms}$ reproduces all observed rise and decay data for these frequencies. We note that the birefringence Δn stemming from the electro-optical Kerr effect is also quadratic in the electric field, $\Delta n \propto E^2$,²⁶

and a very similar rise/decay asymmetry is observed in $\Delta n(t)$ curves.²⁷⁻³⁰ Given that the quantity $\tau = 0.24$ ms associated with all fits is only 30% larger than the low field Debye time of $\tau_D = 0.18$ ms, we conclude as before that it is the Debye time scale that governs this structural recovery process,^{20,21} not the faster α -relaxation time. With this coincidence of the ring/chain conversion time τ with the Debye time τ_D of 5M3H, the present results are again supportive of the picture in which the fluctuation of the Kirkwood correlation factor g_K is at the origin of the Debye process of monohydroxy alcohols and related liquids.^{1,20,21,31} This is equivalent to fluctuations in the end-to-end distance of the chain or in the ring/chain type structural motif.

Based on the time dependence of the $(\epsilon''_{hi} - \epsilon''_{lo})/\epsilon''_{lo}$ curves in Figs. 4 and 5, we observe that this quantity approaches its steady state level in a monotonic fashion and that this level, $[\epsilon''_{hi}(t \rightarrow \infty) - \epsilon''_{lo}]/\epsilon''_{lo}$, is much smaller than $\Delta_E \ln \Delta \epsilon_D$ or $\Delta_E \ln \tau_D$. This implies that for $\nu \geq \nu_{max}$ the cancellation of $\Delta_E \ln \Delta \epsilon_D$ and $\Delta_E \ln \tau_D$ is effective for all times, not only in the steady state case. This suggests that both amplitude ($\Delta \epsilon_D$) and time constant (τ_D) vary concertedly with time, and furthermore that the Debye time scale changes with the ring/chain composition. In support of this notion and according to the results of Singh *et al.*,²¹ the spectral separation of τ_D and τ_α ($d \ln(\tau_D/\tau_\alpha)/dT = -0.029 \text{ K}^{-1}$) and the relaxation amplitude ($d \ln(\Delta \epsilon)/dT = -0.046 \text{ K}^{-1}$) are similar regarding their sensitivity to temperature. When a high dc field is applied, these two quantities also change by similar relative amounts, i.e., $d \ln(\tau_D/\tau_\alpha)/dE \approx d \ln(\Delta \epsilon)/dE$, see Figs. 2 and 3. As a result, when g_K changes with temperature as a consequence of an altered ring/chain equilibrium, not only will the amplitude $\Delta \epsilon_D$ change but also the spectral separation of time constants, $\log(\tau_D/\tau_\alpha)$. We hypothesize that this feature is at the origin of the distinct temperature dependences of $\tau_D(T)$ and $\tau_\alpha(T)$ that seems more pronounced when g_K varies considerably with T .

Finally, we assess the extent to which other known sources of non-linear dielectric behavior contribute to the present findings. Heating related effects can lead to considerable nonlinearities in the case of ac fields,^{32,33} but are suppressed in the present experiments on the basis of the static nature of the high electric field. A recently recognized source of a field induced change in relaxation time is due to the change in entropy that occurs at high fields, $\Delta_E S = \frac{1}{2} \epsilon_0 \nu (\partial \epsilon_s / \partial T) \times E_B^2$, where ν is the molar volume.^{22,24,25,34} A study of various monohydroxy alcohols has shown that $\Delta_E \ln \tau_D$ is approximately proportional to $\Delta_E S$. For 6M3H the results were $\Delta_E \ln \tau_D = 1.48\%$ and $\Delta_E S = -90 \text{ mJ K}^{-1} \text{ mol}^{-1}$ at $T = 195 \text{ K}$ and $E_B = 200 \text{ kV cm}^{-1}$. For 5M3H at $T = 203 \text{ K}$ and $E_B = 171 \text{ kV cm}^{-1}$, $\Delta_E S = -35 \text{ mJ K}^{-1} \text{ mol}^{-1}$ is obtained based on $\partial \epsilon_s / \partial T = -0.17 \text{ K}^{-1}$ and assuming equal molar volumes, $\nu_{5M3H} = \nu_{6M3H}$. Therefore, an entropy effect of $\Delta_E \ln \tau_D = 0.57\%$ is estimated for 5M3H, less than 5% of the observed chemical effect. Similarly, dielectric saturation could counteract the present “chemical” effect observed as positive $\Delta_E \ln \Delta \epsilon_D$, but saturation at these fields tends to remain a $\Delta \epsilon$ reduction of not more than 0.5%. In conclusion, we are confident that the large field effect of this study is dominated by the field driven ring/chain conversion.

V. SUMMARY AND CONCLUSION

The monohydroxy alcohol 5-methyl-3-heptanol near $T = 200 \text{ K}$ is selected for a high dc bias field dielectric study because its Kirkwood correlation factor ($g_K \approx 1$) indicates the coexistence of ring- and chain-like structures with similar free energies. As realized earlier,²⁰ this situation gives rise to a strong sensitivity of structure and dynamics to an electric field, since rings and chains differ considerably in their net dipole moments. In contrast to the earlier approach to 5M3H based upon high ac fields,²¹ employing steps in a dc bias field of sufficient magnitude allows us to directly observe the time dependence of the field induced changes in structure and dynamics.

Steady state spectra of the quantities that gauge the relative changes in permittivity, $(\epsilon'_{hi} - \epsilon'_{lo})/(\epsilon'_{lo} - \epsilon_\infty)$ and $(\epsilon''_{hi} - \epsilon''_{lo})/\epsilon''_{lo}$, are analyzed and the observations are consistent with changes in both the amplitude ($\Delta_E \ln \Delta \epsilon_D = +11.0\%$) and time constant ($\Delta_E \ln \tau_D = +12.6\%$) of the Debye process. The similarity of the two percentage change values leads to a cancellation effect at frequencies $\nu > \nu_{max}$, such that the high frequency sides of the dielectric spectra appear field invariant. The evolutions of these field induced changes are observed as a function of time after applying and after removing the high dc bias field. The resulting rise and decay curves are asymmetric, with the rise always appearing slower than the decay counterpart, analogous to observations for other non-linear dielectric effects^{24,25} and for electro-optical Kerr effect curves.^{27,28} The quadratic field dependence of the steady state effects, $\Delta_E \ln \Delta \epsilon_D \propto E_B^2$ and $\Delta_E \ln \tau_D \propto E_B^2$, implies that squared exponential approaches, $[1 - \exp(-t/\tau)]^2$ and $[\exp(-t/\tau)]^2$, should represent the rise and decay behavior. We find that this quadratic approach captures the observed rise/decay asymmetries, and that all transitions are associated with the same time constant of $\tau = 0.24$ ms, only 30% higher than the Debye time constant, $\tau_D = 0.18$ ms. We conclude that it is the fluctuation of the end-to-end vector of the hydrogen-bonded structures that gives rise to the Debye process, more akin to a fluctuation of the magnitude of a dipole moment (of g_K) rather than the reorientation of a permanent dipole.

The observation that the Debye time scale τ_D is also a matter of the ring/chain equilibrium constant can help to understand the common feature that the Debye process fails to track the temperature dependence of the α -process of monohydroxy alcohols. In other words, the spectral separation of the Debye- and α -peaks, $\log(\tau_D/\tau_\alpha)$, depends on temperature in these liquids. The present study suggests that $\log(\tau_D/\tau_\alpha)$ will change whenever g_K displays a considerable sensitivity to temperature, which is a common feature of monohydroxy alcohols in their viscous regime.¹⁵

¹R. Böhmer, C. Gainaru, and R. Richert, *Phys. Rep.* **545**, 125 (2014).

²S. S. N. Murthy, *J. Phys. Chem.* **100**, 8508 (1996).

³L.-M. Wang and R. Richert, *J. Phys. Chem. B* **109**, 11091 (2005).

⁴L.-M. Wang and R. Richert, *J. Chem. Phys.* **123**, 054516 (2005).

⁵C. Gainaru, T. Hecksher, N. B. Olsen, R. Böhmer, and J. C. Dyre, *J. Chem. Phys.* **137**, 064508 (2012).

⁶C. Gainaru, S. Bauer, E. Vynokur, H. Wittkamp, W. Hiller, R. Richert, and R. Böhmer, *J. Phys. Chem. B* **119**, 15769 (2015).

- ⁷W. Huang and R. Richert, *J. Phys. Chem. B* **112**, 9909 (2008).
- ⁸J. S. Hansen, A. Kisliuk, A. P. Sokolov, and C. Gainaru, *Phys. Rev. Lett.* **116**, 237601 (2016).
- ⁹H. Huth, L.-M. Wang, C. Schick, and R. Richert, *J. Chem. Phys.* **126**, 104503 (2007).
- ¹⁰S. S. N. Murthy and M. Tyagi, *J. Chem. Phys.* **117**, 3837 (2002).
- ¹¹L.-M. Wang, Y. Tian, R. Liu, and R. Richert, *J. Chem. Phys.* **128**, 084503 (2008).
- ¹²T. A. Litovitz and G. E. McDuffie, *J. Chem. Phys.* **39**, 729 (1963).
- ¹³B. Jakobsen, C. Maggi, T. Christensen, and J. C. Dyre, *J. Chem. Phys.* **129**, 184502 (2008).
- ¹⁴C. Hansen, F. Stickel, T. Berger, R. Richert, and E. W. Fischer, *J. Chem. Phys.* **107**, 1086 (1997).
- ¹⁵C. J. F. Böttcher, *Theory of Electric Polarization* (Elsevier, Amsterdam, 1973), Vol. 1.
- ¹⁶P. Bordewijk, F. Gransch, and C. J. F. Böttcher, *J. Phys. Chem.* **73**, 3255 (1969).
- ¹⁷G. P. Johari, O. E. Kalinovskaya, and J. K. Vij, *J. Chem. Phys.* **114**, 4634 (2001).
- ¹⁸W. Dannhauser, *J. Chem. Phys.* **48**, 1911 (1968).
- ¹⁹H. Fröhlich, *Theory of Dielectrics* (Clarendon, Oxford, 1958).
- ²⁰L. P. Singh and R. Richert, *Phys. Rev. Lett.* **109**, 167802 (2012).
- ²¹L. P. Singh, C. Alba-Simionesco, and R. Richert, *J. Chem. Phys.* **139**, 144503 (2013).
- ²²S. Samanta and R. Richert, *J. Chem. Phys.* **142**, 044504 (2015).
- ²³S. Havriliak and S. Negami, *Polymer* **8**, 161 (1967).
- ²⁴A. R. Young-Gonzales, S. Samanta, and R. Richert, *J. Chem. Phys.* **143**, 104504 (2015).
- ²⁵S. Samanta, O. Yamamuro, and R. Richert, *Thermochim. Acta* **636**, 57 (2016).
- ²⁶M. S. Beevers, D. A. Elliott, and G. Williams, *J. Chem. Soc., Faraday Trans. 2* **76**, 112 (1980).
- ²⁷R. Coelho and D. Khac Manh, *C. R. Acad. Sci. Paris Ser. C* **264**, 641 (1967).
- ²⁸J. Crossley and G. Williams, *J. Chem. Soc., Faraday Trans. 2* **73**, 1906 (1977).
- ²⁹M. S. Beevers, J. Crossley, D. C. Garrington, and G. Williams, *Faraday Symp. Chem. Soc.* **11**, 38 (1977).
- ³⁰J. Crossley and G. Williams, *J. Chem. Soc., Faraday Trans. 2* **73**, 1651 (1977).
- ³¹C. Gainaru, R. Meier, S. Schildmann, C. Lederle, W. Hiller, E. A. Rössler, and R. Böhmer, *Phys. Rev. Lett.* **105**, 258303 (2010).
- ³²W. Huang and R. Richert, *J. Chem. Phys.* **130**, 194509 (2009).
- ³³R. Richert, *Adv. Chem. Phys.* **156**, 101 (2014).
- ³⁴G. P. Johari, *J. Chem. Phys.* **138**, 154503 (2013).